SAE Aerospace
An SAE International Group

AEROSPACE INFORMATION REPORT

SAE AIR1935

Issued 1985-02
Reaffirmed 2007-11

Methods of Controlling Distortion of Inlet Airflow During Static Acoustical Tests of Turbofan Engines and Fan Rigs

1. INTRODUCTION: Generally it is desirable during static engine noise testing to simulate the noise-generating processes that occur during takeoff or landing. One factor that may have significant influence on fan noise from turbofan engines during static testing is the airflow distortion encountered by the low-pressure fan stage. This report presents technical details on devices that "condition" the airflow entering the engine to more nearly simulate flight operations without introducing a detrimental impact on sound propagating from the engine.

Noise generated by the fan component of a non-inlet-guide-vane turbofan engine operating statically can be significantly different than when operating with forward velocity, i.e., during flight operation or in a wind tunnel. When operated statically, the airflow into the engine has higher levels of both steady and unsteady distortions. As a result the fan may generate noise levels higher than would be observed at equivalent engine power settings in flight. The higher noise levels are more likely to occur in the case of turbofan engines with a single stage fan operating at conditions where the blade passing frequency has been designed to be acoustically cut-off. This normally occurs at approach power. Reference 1 cites some of the early observations of static and flight noise differences and offers possible explanations. A summary of observations on static noise testing as deduced from industry and government sponsored research programs as of the mid 1970's is provided in Reference 2.

A schematic representation of the stream of airflow into an inlet for the static and flight situations is provided in Figure 1. The flight situation is visualized as one in which the inflow is captured in a slightly contracted stream tube (see Figure 1(b)).

Static engine operation is visualized as a sink type flow, see Figure 1(a). For the flight situation, the sound pressure level of the fan tone that results from ingestion of normal levels of atmospheric turbulence has been shown to be small. This conclusion is based on the analytical studies presented in References 3 and 4. There are several sources of distortion during static operation: they include atmospheric turbulence, vorticity caused by flow over the engine test stand structure, and vorticity generated by the presence of the ground plane. Atmospheric turbulence can be generated by wind gusts, thermal gradients, flow over local terrain, (e.g., hills, trees, buildings), and reingestion of exhaust flow. The effect of the large contraction of the static flow field on atmospheric turbulence and inducement of flow over and around the test stand structure can cause significant distortion in the flow entering the fan. Noise can be produced by interactions between the rotating fan blades and the distorted airflow. The level of noise that can be generated depends upon the fan stage design, engine power setting and the local environmental conditions. Some fan stage designs are such that there may be negligible extraneous noise developed by inflow distortion.

2. PURPOSE: To describe the principal design features of devices that help to simulate flight inflow conditions during static noise testing of a turbofan engine.

3. SCOPE: This Aerospace Information Report provides guidelines for hardware design. Guidelines on such items as engine types, test arrangements, and test purposes that would benefit from the use of an inflow control device during static noise testing are outside the scope of this report.

4. APPLICATIONS: Techniques similar to those used in wind tunnel design have been applied to develop devices to condition the flow that enters the inlet of an engine. These inflow control devices (ICDs) are made of turbulence suppressing material such as honeycomb, perforated plate, or wire mesh. The devices generally have closed geometric shapes tending toward spheres so that the flow is nearly perpendicular to the ICD surface. Some ICDs have been installed inside an inlet (see Figure 2, ICD No. 2), but test results have shown an undesirable impact on the forward-radiated sound field and loss of inflow total pressure (Ref. 5). Test data suggest that an ICD performs best when the diameter is about 1.5 or more times the fan diameter. Schematics of the various ICDs for which information was available are shown in Figure 2. Table 1 provides a list of design parameters for ICDs that have been tested. Photographs or schematics and discussions of experimental results can be found in References 5 to 9.

5. REVIEW OF TEST RESULTS: Figure 3 provides a summary assessment of inflow distortion under static and flight conditions, both with and without an ICD. The data were obtained from pressure transducers mounted at various radial locations near the leading edge of a fan rotor blade of a high-bypass-ratio turbofan engine. The static testing was accomplished on an outdoor test stand. The flight configuration was an under-wing engine installation. The transducers were mounted on the pressure surface of the blades, and the radial locations were such that the measurements represent 1) the flow within the inlet wall boundary layer (at 98% radius), 2) the transition region between the boundary layer and the freestream (at 96% radius), and 3) the freestream flow (at 92% radius). Since the transducers responded to any

pressure fluctuation that reached the blade surface regardless of the origin, the results must be carefully interpreted (pressure fluctuations on the blade are assumed to represent distortion of the inlet flow). Figure 3 shows that at 92% radius, the distortion present in the static case without inflow control was reduced by the ICD to a level which resulted in blade surface pressures that were in very good agreement with those measured during flight. At 96% and 98% radius there was better agreement when the static data were measured with an ICD; however, the flight situation had even less distortion. On the basis of the data in Figure 3 and other data, it was concluded that use of an inflow control device for static testing can provide a significant reduction in inflow distortion.

An assessment of the transmission of acoustic signals propagating through inflow control devices Nos. 1 to 5 of Figure 2 is reported in Ref. 5. Reference 5 concluded that ICD No. 2 caused significant sound transmission loss when the mean Mach number at the ICD surface (neglecting blockage) was less than approximately 0.12. The smallest ICDs (Nos. 3 and 4) exhibited small transmission loss when the Mach number of the flow through the ICD reached approximately 0.15. Evaluation of ICDs Nos. 6 and 7 of Figure 2 can be found in Refs. 6 and 7, respectively. Both reports concluded that acoustic transmission loss was negligible. Data for ICD No. 8 are provided in Figure 4. The data were obtained by placing a loudspeaker in an engine inlet to provide a constant level noise source. The radiation patterns for a wide frequency range showed small variations. The variations were within estimated test accuracy implying negligible transmission loss within the frequency range of interest. From all observations combined, it was concluded that inflow control devices can be designed such that sound propagating to the far-field is not significantly affected by transmission through an ICD.

Table 2 provides a summary of differences between the sound pressure level in the 1/3-octave band containing the blade-passing frequency from flyover noise measurements and from static data projected to flight (see Reference 10 for details). The static data were obtained both with and without an ICD and demonstrated the benefit of the ICD. The data shown in Table 2 were obtained from an engine designed for cutoff of the interaction between fan rotor and downstream stator. (Because of the cut-off design the sound pressure level of the 1/3 octave band containing the blade-passing frequency has the greatest sensitivity to inflow distortion.) The data in Table 2 were derived from data similar to that shown in Figure 5 where the static data projected to flight are compared with flight data for various directivity angles. Fan tip relative Mach number is also listed in Table 2 because it is a parameter of relevance to noise generation. Overall, testing without an inflow control device has been observed to produce significantly higher sound levels than measured in flight. With an inflow control device installed, the static-to-flight sound pressure level differences were significantly reduced.

6. REVIEW OF DESIGN DATA: A relatively wide range of ICD designs is shown in Figure 2. Some of the physical characteristics of the designs are shown in Table 1.

Treating the ICDs as approximately spherical objects to estimate an equivalent diameter as the basis to calculate a ratio of ICD diameter to engine fan diameter shows that the ICDs ranged generally from two to four fan diameters in size when installed on the largest engine for which they were designed. The ratio of honeycomb cell thickness to cell diameter listed in Table 1 is the design parameter that varied the most in different designs. This parameter primarily affects the suppression of transverse velocity fluctuations and has a value ranging between approximately 2 and 12 for the listed ICDs. The high values appear to be overly conservative. All of the designs incorporated either perforated plate or wire mesh (located on either side of the honeycomb) with approximately 40 to 50 percent open area as the material for suppression of the axial velocity fluctuations.

A method to calculate the values of design parameters for an ICD has been developed and is reported in References 10 and 11. Table 3 compares design values calculated by the Reference 10 method with values for ICD Nos. 8 and 11. These two ICDs were designed prior to the publications of References 10 and 11. The most obvious differences is that the design method of References 10 and 11 suggests that a much smaller ratio of honeycomb cell thickness-to-diameter could have been used. While ICD Nos. 8 and 11 have been successful, other ICDs listed in Table 1 also have demonstrated success with thickness-to-diameter ratios closer to that suggested by the design method. Thus, future ICD designs should consider the design method of References 10 and 11 as well as the designs of existing ICDs that have demonstrated success.

The most difficult step in applying the design method of References 10 and 11 may be that of quantifying the turbulence and steady distortion that exists in the static and flight inflow capture areas. Flow field measurements in the vicinity of the inlet provide the best starting point. It should also be recognized that flow distortion can vary randomly and rapidly. For example, changes in wind speed or wind direction can affect either the fan-ingested distortion caused by flow around test stand structural elements or the scale and intensity of the atmospheric turbulence.

Two additional important considerations are: (1) clearance between the bottom of the ICD and the ground plane and (2) mating of the ICD to the engine. Sufficient ground clearance should be provided so as to not encounter significant flow distortions as a result of proximity to the ground plane boundary layer. Successful ICDs typically have ground clearances of at least one-eighth the ICD diameter. ICD installations with clearance less than one-eighth the ICD diameter should be checked experimentally to ensure that undesirable air flow distortion is not present. Similar care and checkout of the system used to mate the ICD to the engine structure is required. Distortion can be generated when there are small, non-uniform gaps through which air can flow at the junction between the ICD and the engine. Gaps occur when there is movement of the engine or inlet due to thrust or pressure loads, especially if movement is available by design to accommodate the possibility of engine surge. In this respect, selection of the inlet lip design (i.e., a flight inlet or a bellmouth fairing into the flight inlet) should consider the presence of the ICD.

7. CONCLUDING REMARKS: Inflow control devices comprised of honeycomb and perforated plate or honeycomb and wire mesh have been developed and successfully used for acoustical testing of turbofan engines and fan rigs operated statically. Without ICDs the fan may ingest flow that is distorted resulting in an extraneous source of noise which in many cases produces higher sound pressure levels than occur during flight operation.

Scaling of the ICD design values shown in Table 1 and/or using the design method of References 10 and 11 should result in an inflow control device that will provide noise-generating conditions during static engine operation approaching those that would be observed in flight.

PREPARED BY THE
GAS TURBINE PROPULSION SUBCOMMITTEE
OF SAE COMMITTEE A-21, AIRCRAFT NOISE

REFERENCES

1. Cumpsty, N. A. and Lowrie, B. W., "The Cause of Tone Noise Generation by Aeroengine Fans at High Subsonic Tip Speeds and the Effect of Forward Speed," ASME Paper 73-WA/GT-4, Detroit, Mich., 1973.

2. Feiler, C. E. and Groeneweg, J. F., "Summary of Forward Velocity Effects on Fan Noise," AIAA Paper 77-139, October, 1977.

3. Ganz, U. W., "Analytical Investigation of Fan Tone Noise due to Ingested Atmospheric Turbulence," NASA CR 3302, August, 1980.

4. Gliebe, P. P., "Analytical Study of the Effects of Wind Tunnel Turbulence on Turbofan Rotor Noise," AIAA Paper No. 80-1022P, June 1980, Journal of Aircraft Vol. 18, No. 10, October, 1981, pp. 818-825.

5. McArdle, J. G., Jones, W. L., et al, "Comparison of Several Inflow Control Devices for Flight Simulation of Fan Tone Noise Using a JT15D-1 Engine," AIAA Paper 80-1025, June, 1980.

6. Ho, P. Y., Smith, E. B., and Kantola, R. A., "An Inflow Turbulence Reduction Structure for Scale Model for Testing," AIAA Paper 79-0655, March, 1979.

7. Lowrie, B. W. and Newby, D. R., "The Design and Calibration of a Distortion-Reducing Screen for Fan Noise Testing," AIAA Paper 77-1323, October, 1977.

8. Atvars, Y. and Rogers, D. F., "The Development of Inflow Control Devices for Improved Simulation of Flight Noise Levels during Static Testing of a HBPR Turbofan Engine," AIAA Paper 80-1024, June, 1980.

9. Rogers, D. F. and Ganz, U. W., "Aerodynamic Assessment of Methods to Simulate Flight Inflow Characteristics during Static Engine Testing," AIAA Paper 80-1023, June, 1980.

10. Peracchio, A. A., Ganz, U. W., et al, "Studies on Proper Simulation during Static Testing of Forward Speed Effects on Fan Noise," NASA CR 165626, Sept. 1980.

11. Peracchio, A. A., "Assessment of Inflow Control Structure Effectiveness and Design System Development," Journal of Aircraft, Volume 19, No. 12, December, 1982.

TABLE 1: **DESIGN PARAMETERS OF INFLOW CONTROL DEVICES**

Company-Application	ICD Approximate Diameter (meters)	ICD Dia./ Fan Dia. (Ratio)	Honeycomb		Perforated Plate or Wire Mesh Parameters* (Turbulence Suppression Material)
			Cell Diameter (mm)	Thickness/ Cell Dia. (Ratio)	
P&WA - No. 11*** HPBR Engines	7.32	3.1	9.5	8	Perf. Plate: 4.8, .65, 51
Boeing - No. 8 HPBR Engines	7.32	3.1	3.2	12	Perf. Plate: 1.59, .50, 46
Boeing - No. 10 Scale Models	1.14	3.75	6.3**	4	Perf. Plate: 1.59, .50, 46 Wire Mesh: .46, 6.3
Rolls Royce - Scale Models and Small HBPR Engine - No. 9	2.03	2.35	6.3	2	Wire Mesh: .91, 3.9
General Electric - Scale Models - No. 6	2.09	4.1	6.3	8	Wire Mesh: .91, 3.9
NASA-Lewis - Scale Models and Small HBPR Engine	.85 2.13	1.7 4.2	6.3 6.3	4 8	See Figure 2, Nos. 1,3,4,5
SNECMA - Scale Models - No. 7	1.50	3.2	3.2	3.2	Wire Mesh: .32, 7.9

* Perforated Plate parameters: Hole Diameter (mm), Sheet Thickness/Hole Dia., Open Area Ratio (%).
Wire Mesh parameters: Wire Diameter (mm), Wires/cm

** Estimated equivalent value

*** Refers to number on Figure 2

TABLE 2: **DIFFERENCES BETWEEN MEASURED FLYOVER SOUND PRESSURE LEVELS AND SOUND PRESSURE LEVELS PROJECTED FROM MEASUREMENTS AROUND A STATIC ENGINE**

FLIGHT CONDITION	Static Data Without Inflow Control	Static Data With Inflow Control
	ΔSPL (σ), dB	SPL (σ), dB
Approach 30° Flap ($M_T \approx 0.89$)	-3 (1.7)	1.2 (1.6)
Approach 25° Flap ($M_T \approx 0.90$)	-4.5 (1.4)	-0.1 (1.4)
TAKEOFF ($M_T \approx 1.26$)	-3.2 (1.5)	-1.8 (2.3)
CUTBACK ($M_T \approx 1.17$)	-5.0 (2.7)	-2.6 (2.3)
AVERAGE OVER ALL ANGLES AND POWER SETTINGS	-3.9 (2.04)	-0.8 (2.4)

NOTE: M_T = Fan relative tip Mach number

ΔSPL, dB = Flight data minus static projected data (for the 1/3 octave band containing blade passing frequency)

σ = Standard deviation of ΔSPL

See Figure 5 for details of correlations between in-flight sound pressure level measurements and sound pressure levels projected from static-engine data.

TABLE 3: **DESIGN PARAMETERS FOR INFLOW CONTROL DEVICES**

PARAMETER	DESIGN SYSTEM (REF. 10)	P&WA LARGE ICD FIG. 2; NO. 11	BOEING LARGE ICD FIG. 2; NO. 8
NOMINAL ICD RADIUS, m	3.47	3.66	3.66
DETAIL DIMENSION (HONEYCOMB CELL DIA.), mm	6.7	9.5	3.2
DETAIL DIMENSION (PERFORATED-PLATE HOLE DIA.) mm	3.0	4.8	1.59
RATIO OF CELL THICKNESS/DIAMETER	1.7	8.0	12.0
OPEN AREA RATIO (PERFORATED PLATE), %	54	51	46

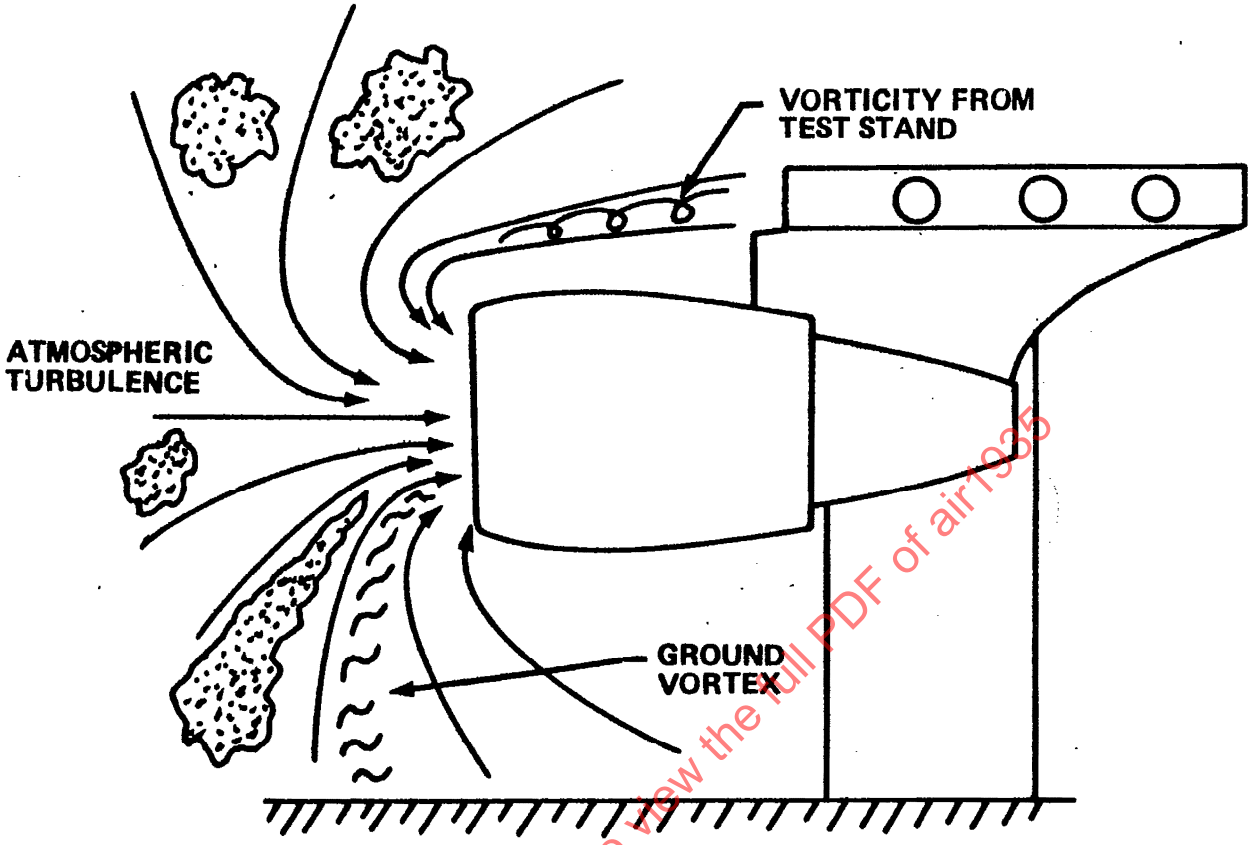

(a) GROUND STATIC TEST

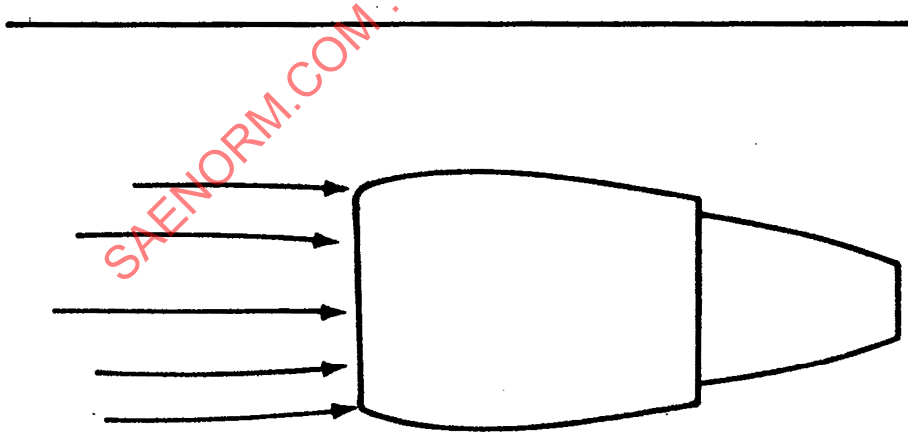

(b) FLIGHT

FIGURE 1 SCHEMATIC OF INFLOW FOR STATIC AND FLIGHT

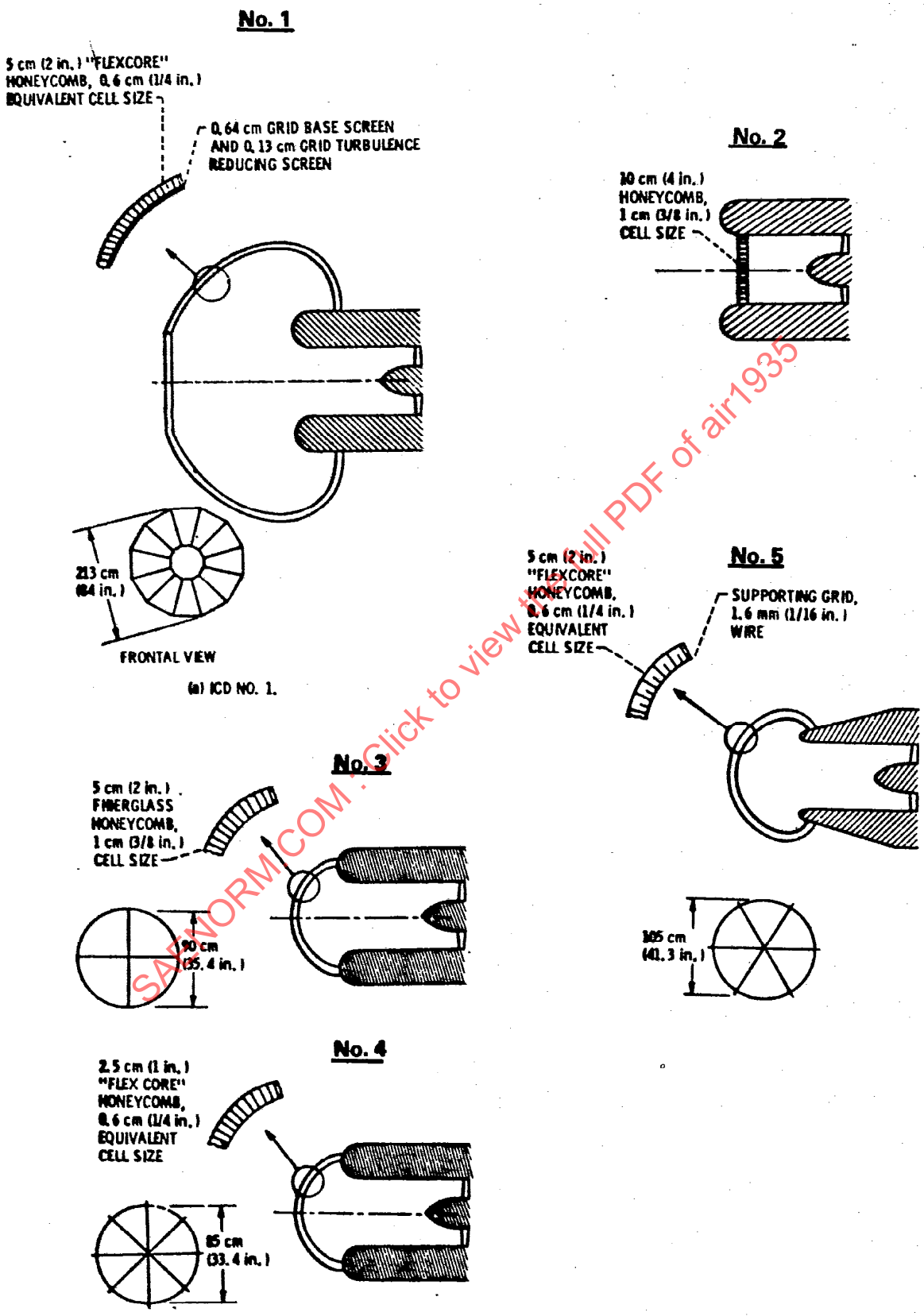

FIGURE 2. INFLOW CONTROL DEVICES THAT HAVE BEEN TESTED (REFER TO TABLE 1 FOR DETAILS)

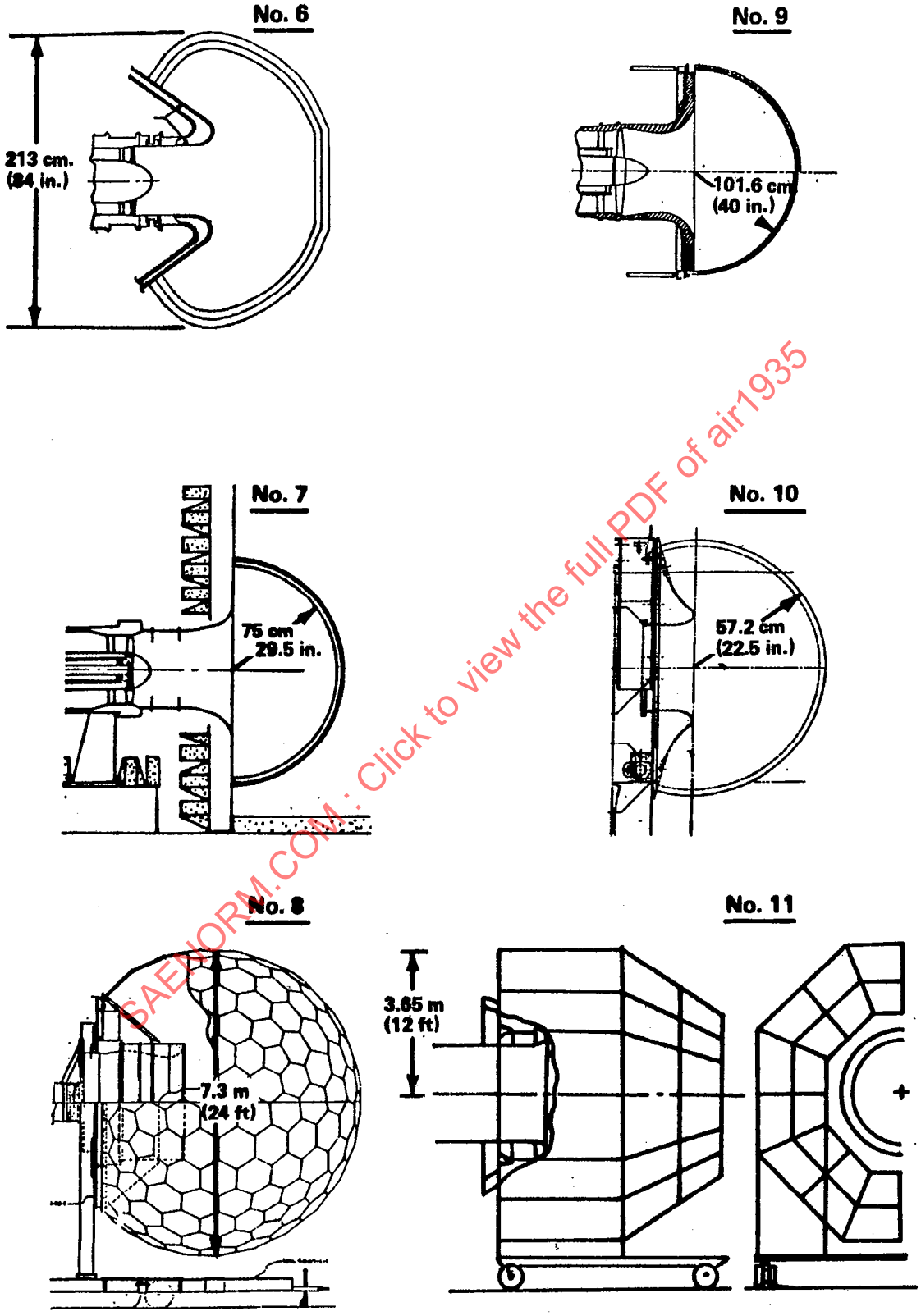

FIGURE 2. (concluded)